ORAL REFERENCE: ICF100877OR

OBSERVATION OF FATIGUE CRACK INITIATION AND EARLY PROPAGATION IN ULTRAFINE-GRAINED STEEL BY ATOMIC FORCE MICROSCOPY

H. Kimura [1], Y. Akiniwa [2], K. Tanaka [2], J. Kondo [1] and T. Ishikawa [3]

[1] Graduate School, Nagoya University,
Furo-cho, Chikusa-ku, Nagoya 464-8603, Japan
[2] Department of Mechanical Engineering, Nagoya University,
Furo-cho, Chikusa-ku, Nagoya 464-8603, Japan
[3] Steel Research Laboratories, Technical Development Bureau, Nippon Steel Corporation,
20-1 Shintomi, Futtsu-city, Chiba 293-8511, Japan

ABSTRACT

Steel plates produced by an advanced thermo-mechanical control process have two regions: the ultrafine-grained surface layer with the average grain size of less than 2 μm and the intermediate region with medium-sized grains. Smooth specimens of the ultrafine and medium-sized grains were prepared to conduct fatigue tests under cyclic axial tension compression at room temperature. The effect of the microstructure on the fatigue crack initiation as well as the early propagation behavior was investigated by observing images of specimen surfaces replicated on plastic sheets by atomic force microscopy. In the specimens of the medium-sized grains, the fatigue cracks initiated from the simple straight slip lines. In the ultrafine-grained specimens, complex slip deformation in the shape of irregularities of the specimen surface was observed prior to the initiation of fatigue cracks. The initiation of fatigue cracks was observed at the grain boundary between the grains containing the complex slip deformation at an early stage of fatigue cycles. The crack propagation rate in the ultrafine-grained specimens decreases because of the crack deflection, bifurcation and the grain-boundary blocking at an early stage of the propagation.

KEYWORDS

ultrafine-grained steel, fatigue, crack initiation, crack propagation, microstructure, atomic force microscopy

INTRODUCTION

Steel plates with ultrafine-grained surface layers, called SUF plates, exhibit excellent crack arrestability against brittle fracture. They have already been put into practical use as the structural components of ships to prevent them from unexpected catastrophic fracture [1]. SUF plates are produced by an advanced thermo-mechanical control process to yield ultrafine-grained surface layers with the average grain size of less than 2 μm and relatively coarse microstructure in the intermediate region. Though the fatigue properties of SUF plates are also expected to be excellent [2,3], the mechanism of the improvement especially in the ultrafine-grained surface layer has not yet been clarified. Atomic force microscopy (AFM) will be a powerful tool to investigate the crack initiation process because the size of ultrafine grains is so small that it is difficult to observe the plastic sheets replicated from the specimen surface by scanning electron microscopy (SEM). AFM observations make it possible to study the fatigue crack initiation process based on the three-dimensional measurement of the specimen surface [4-6].
In this study, fatigue tests were conducted on the specimens prepared from the ultrafine-grained surface layer and the medium-grained intermediate region. The effect of the microstructure on the fatigue crack initiation as well as the early propagation behavior was investigated by AFM.

EXPERIMENTAL PROCEDURE

The advanced thermo-mechanical control process where accelerated cooling during the rolling of steel plates was followed by controlled rolling in the reheating process was employed to yield ultrafine grains on the surface layers with the thickness of 7 mm on the both sides of a 50-mm-thick plate. Chemical compositions of the basic components are 0.11wt%C, 0.20wt%Si, 1.44wt%Mn, 0.007wt%P and 0.005wt%S. The SEM images of the electrolytically polished specimen surfaces of the ultrafine-grained surface layer and the medium-grained intermediate region are shown in Fig. 1. The surface layer consists of ferrites and cementites dispersed at grain boundaries [7], whereas the intermediate region is composed of ferrites and pearlites. The mechanical properties and grain size are presented in Table 1. Grain sizes d_S, d_T and d_L correspond to the average grain length parallel to the axes S, T and L shown in Fig. 2 respectively. Specimens were prepared from the surface layer and intermediate region with the rolling direction parallel to the loading axis by electrical discharge machining followed by electrolytic polishing.

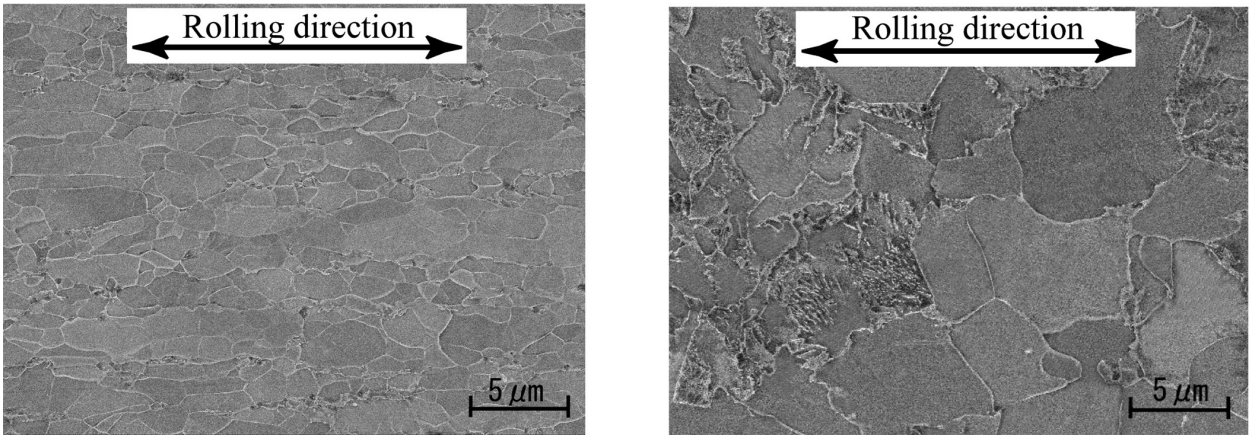

(a) Ultrafine-grained surface layer (b) Medium-grained intermediate region

Fig. 1. Specimen surfaces finished by electrolytic polishing.

Table 1 Mechanical properties and grain size.

Material	Mechanical properties (MPa)			Grain sizes (μm)		
	σ_Y	σ_B	σ_{W0}	d_S	d_T	d_L
Ultrafine-grained	463	537	285	1.8	3.1	4.5
Medium-grained	386	488	245	6.7	9.6	8.6

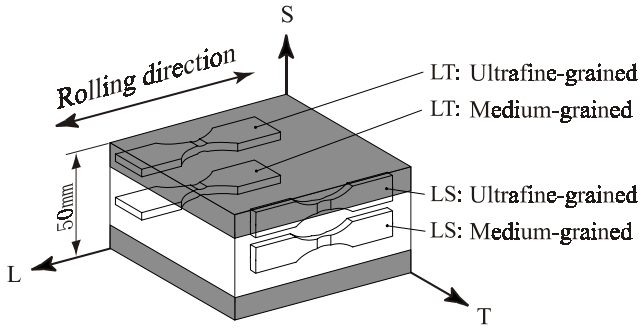

Fig. 2. Specimen orientation.

Smooth specimens were fatigued under cyclic axial loading with the stress ratio R=-1 in air at room temperature. The both sides of the specimen surface were replicated with cellulose acetate sheets under the maximum and minimum applied stresses. The observations were made on the cellulose acetate sheets by AFM and SEM. The AFM images presented in this paper are the images scanned on the cellulose acetate sheets where the grain boundaries are intrusions as opposed to the extrusions on the actual specimen surfaces.

EXPERIMENTAL RESULTS

Crack initiation in the medium-grained specimens

Figure 3 shows the AFM images of the replicated surface of the medium-grained L-S specimen under the maximum applied stress of σ_{max}= 250 MPa. The number of cycles at fracture N_f was 9.2×10^5. The uppercase letter "A" in the figure indicates a grain, whereas the lowercase letter "a" denotes the location of slip lines in the grain. The image in (a) is the one before the fatigue test. In the image at $N/N_f = 2.2\times10^{-2}$ in (b), slip lines at the location of M1a had initiated in the grain M1A and other slip lines were also clearly observed on the left of M1A. Those slip lines with the angle of approximately 45 degrees from the loading axis finally merged to form the main crack.

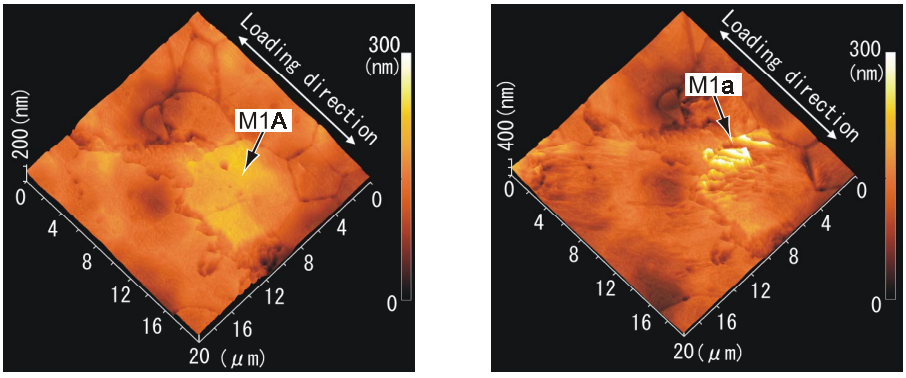

(a) $N/N_f = 0$ (b) $N/N_f = 2.2\times10^{-2}$

Fig. 3. AFM images of crack initiation (Medium-grained, σ_{max} = 250 MPa, $N_f = 9.2\times10^5$).

Crack initiation in the ultrafine-grained specimens

Figure 4 shows the scanning electron micrographs of the surface of the ultrafine-grained specimen fatigued under σ_{max} = 290 MPa up to N =2.6×10^5 with N_f =3.8×10^5. The image in (a) shows simple slip lines. The image in (b) shows the complex slip deformation in the shape of irregularities of the surface in contrast with the simple straight slip lines. This complex slip deformation was rarely observed on the medium-grained specimen surface.

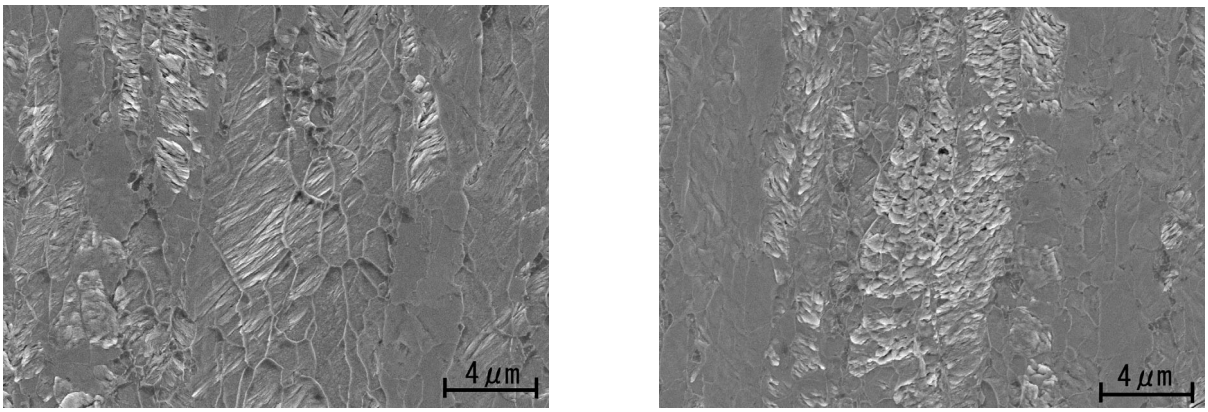

(a) Simple slip lines. (b) Complex slip deformation.

Fig. 4. SEM images of slip deformation (Ultrafine-grained, σ_{max} = 290 MPa, $N = 2.6\times10^5$).

Figure 5 is the AFM images of a crack initiation site. The image in (a) is before the fatigue test. A slip line initiated at U1a in the grain U1A at $N/N_f = 4.0\times10^{-3}$. At $N/N_f = 8.0\times10^{-3}$ in (b), U1b in the grain U1B and U1c in the grain U1A became protrusive due to complex slip deformation. At $N/N_f = 2.1\times10^{-2}$ in (c), the slip line initiated at U1a had propagated through the grain U1A to the opposite grain boundary. Another slip line U1d was formed in U1A. The complex slip deformation U1b in U1B had become more protrusive. The main crack initiated from the grain boundary between U1b and U1c after $N/N_f = 4.2\times10^{-2}$ as shown in (d).

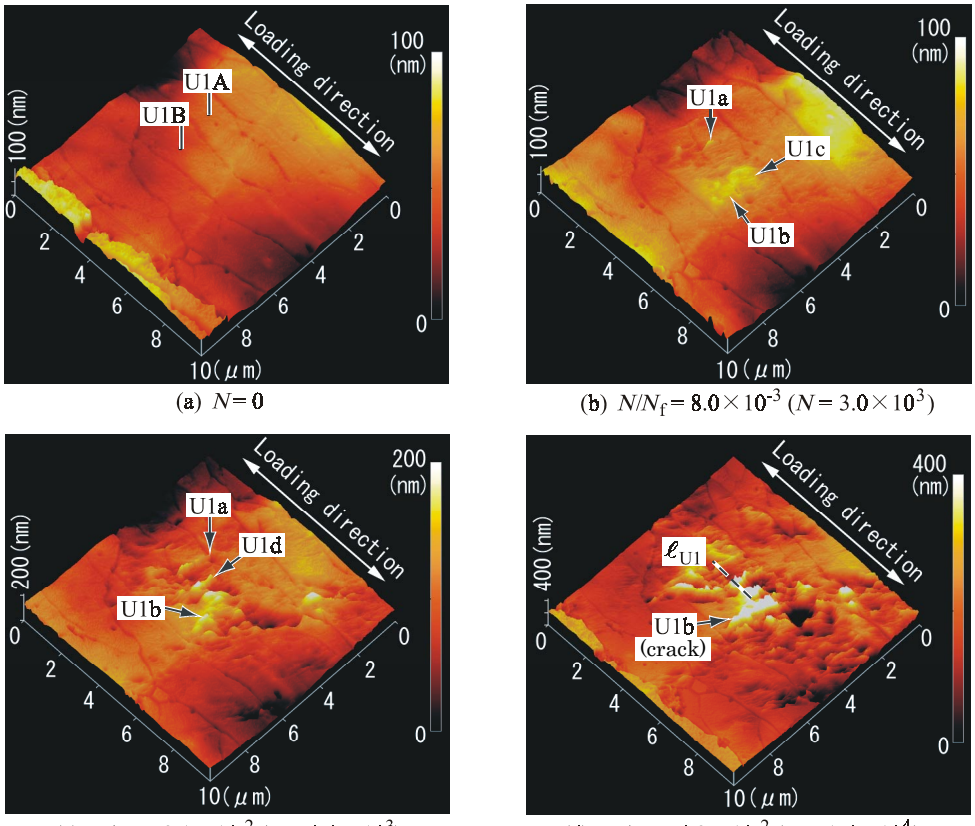

Fig. 5. AFM images of crack initiation (Ultrafine-grained, σ_{max} = 290 MPa, $N_f = 3.8\times10^5$).

Figure 6 (a) shows the change of the sectional profile along the line ℓ_{U1} shown in Fig. 5 (d). The line ℓ_{U1} is perpendicular to slip lines in the grain U1A, where the initiation of the first slip deformation was observed. Figure 6 (b) shows the change of the depth of intrusions, which is the height of extrusions on the replicated plastic sheets, at U1a and U1c. As the number of cycles increased, the depth of intrusion at U1a reached the plateau of 145 nm because it propagated through the grain U1A and came to a standstill at the opposite grain

boundary at $N/N_f = 2.1\times10^{-2}$ as shown in Fig. 5 (c). The depth of intrusion at U1c, however, had a tendency to increase as the number of cycles increased.

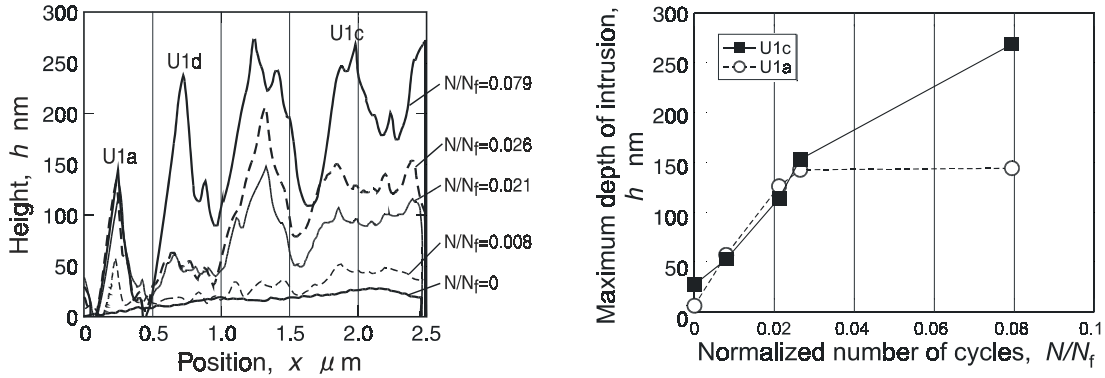

(a) Sectional profiles along the line ℓ_{U1} in Fig. 5(d). (b) Maximum depth of intrusion vs. N/N_f.

Fig. 6. Change of the surface morphology in the fatigue crack initiation process.

Figure 7 shows the AFM images under σ_{max} = 310 MPa with $N_f = 1.9\times10^5$. The image in (a) is before the fatigue test. Slip lines were observed at U3a in the grain U3A and U3b in the grain U3B at $N/N_f = 5.3\times10^{-3}$. The image in (b) was taken at $N/N_f = 1.6\times10^{-2}$. The surfaces of the both grains became irregular due to slip deformation. At $N/N_f = 5.3\times10^{-2}$, one of the slip lines in the grain U3A reached the grain boundary as shown in (c). At $N/N_f = 2.1\times10^{-1}$, a crack initiated from the grain boundary into the grains U3A and U3B as shown in (d). The directions of the crack propagation in those grains were not parallel to the directions of slip lines observed prior to the crack initiation.

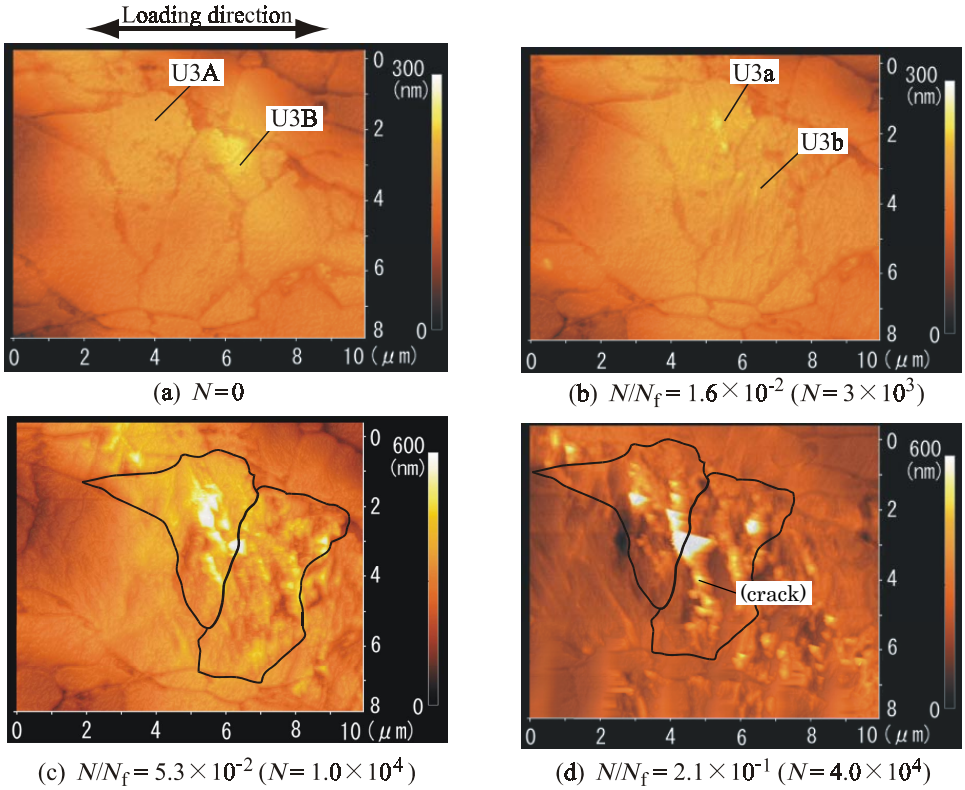

(a) $N=0$ (b) $N/N_f = 1.6\times10^{-2}$ ($N = 3\times10^3$)

(c) $N/N_f = 5.3\times10^{-2}$ ($N = 1.0\times10^4$) (d) $N/N_f = 2.1\times10^{-1}$ ($N = 4.0\times10^4$)

Fig.7. AFM images of crack initiation (Ultrafine-grained, σ_{max} = 310 MPa, $N_f = 1.9\times10^5$).

Fatigue crack propagation at an early stage

Figure 8 shows the relation between crack propagation rate da/dN and the crack-tip position a of the crack shown in Fig. 7 with the corresponding SEM image of the crack superimposed on the AFM image of the surface. The decreases in da/dN at A1 and A2 can be attributed to the deflection of the main crack

perpendicular to the loading axis by colliding into slip lines having initiated before the formation of the main crack with the angel of 60 degrees from the loading axis. The decreases in d*a*/d*N* at the points B1 and B2 are attributed to the blocking of the grain boundaries. In comparison with the case of the surface layer, d*a*/d*N* in the medium-sized grains was relatively larger in spite of the smaller applied stress.

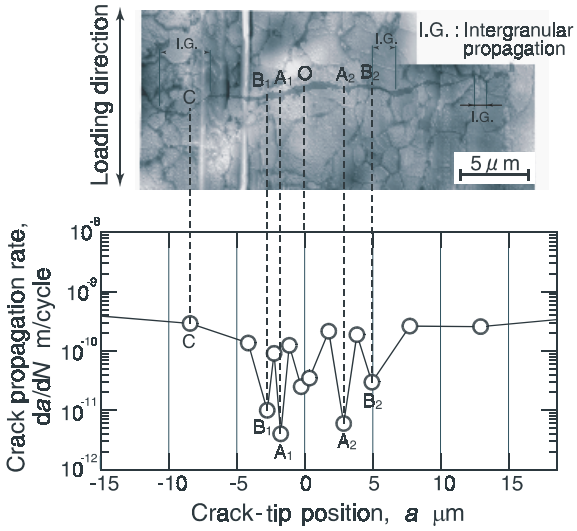

Fig. 8. Relation between crack propagation rate and crack-tip position *a* in ultrafine-grained specimen.

CONCLUSION

Fatigue tests were conducted in the ultrafine-grained and medium-grained specimens. The effect of the microstructure on fatigue crack initiation was investigated. The results are as follows:

(1) Fatigue crack initiation in the ultrafine-grained surface layer is characterized by the formation of complex slip deformation as well as simple slip lines in the grains at an early stage of fatigue cycles. The fatigue cracks initiate at the boundary between the grains with the complex slip deformation. Though simple slip lines were observed in places, none of them led to the formation of the main cracks.

(2) Fatigue crack initiation in the medium-grained specimens is from slip lines. The complex slip deformation formed on the ultrafine-grained specimens was rarely observed.

(3) The comparison of intrusions and extrusions of slip deformation showed no difference under maximum and minimum applied stresses in both ultrafine-grained and medium-grained specimens.

REFERENCES

1. Ishikawa, T., Nomiyama, Y., Hagiwara, Y. et al. (1995) *Materials Engineering*, ASME, New York.
2. Ishikawa, T. (1998) Proc. 24th Symp. Fatigue, The Soci.Mater. Sci., Jpn, 28
3. Kimura, H., Akiniwa, Y., Tanaka, K., Kondo, J. and Ishikawa, T. (2000) Proc. 10th Iketani Conf., 75
4. Nakai, Y., Ohnishi, K. and Kusukawa, T. (1999) Trans. Jpn. Soc. Mech. Eng. , 65-631, 483
5. Yoon, W.K., Inoue, T., Noguchi, H. and Higashide, K. (1998) Trans. Jpn Soc. Mech. Eng. , 64-622, 1435
6. Gerberich, W.W., Harvey S.E., Kramer, D.E. and Hoehn J.W. (1998) Acta Mater., 46-14, 5007
7. Mabuchi, H. and Ishikawa, T. (1997) Proc. Mat. Sol. '97 Accel. Cooling/Direct Quen. Steels, 43